Approach to Control Moment Gyroscope Steering Using Feedback Linearization

John Dzielski*
Pennsylvania State University, State College, Pennsylvania 16804
Edward Bergmann† and Joseph A. Paradiso‡
Charles Stark Draper Laboratory, Cambridge, Massachusetts 02139
and
Derek Rowell§ and David Wormley¶
Massachusetts Institute of Technology, Cambridge, Massachusetts 02139

This paper presents an approach to steering control moment gyroscopes. A technique based on feedback linearization theory is used to transform the original nonlinear problem to an equivalent linear form without approximating assumptions. Under this transformation, the spacecraft dynamics appear linearly, and are decoupled from redundancy in the system of gyroscopes. A general approach to distributing control effort among the available actuators is described that includes provisions for redistribution of rotors, explicit bounds on gimbal rates, and guaranteed operation at and near singular configurations. A particular algorithm is developed for systems of double-gimballed devices, and demonstrated in two examples for which many existing approaches fail to give adequate performance.

Introduction

THERE are a variety of actuators available to generate torques on a spacecraft for the purpose of attitude control. Although propulsive actuators such as reaction control jets are probably the most common, there is another class of actuators that operate by transferring momentum to and from the spacecraft. A control moment gyroscope (CMG) is constructed with a rotor that spins at a constant speed. The rotor is mounted in a gimbal system that can reorient the rotor momentum by rotating the flywheel. CMGs can be used to apply torques to a spacecraft by rotating the angular momentum vectors of the individual rotors. Moving the individual rotors changes the net angular momentum of the group of CMGs. In the absence of external torques, momentum conservation implies a corresponding change in the vehicle momentum, or equivalently, the angular rate of the vehicle. Because CMGs are capable of producing significant torques and can smoothly manipulate large quantities of momentum over long periods of time, they are often favored in precision pointing applications and in momentum management of large, long-duration spacecraft.

In any particular application, control torques are generated by manipulating the momentum stored in a group of CMGs. The net stored momentum is given by a function of the form

$$\boldsymbol{h} = \boldsymbol{h}_{\text{cmg}}(\boldsymbol{\theta}) \tag{1}$$

where $\boldsymbol{h} \in \boldsymbol{R}^3$ is the net CMG momentum vector in a spacecraft-fixed reference frame, $\boldsymbol{\theta} \in \boldsymbol{R}^m$ denotes the set of gimbal displacements, and $\boldsymbol{h}_{\text{cmg}}: \boldsymbol{R}^m \to \boldsymbol{R}^3$ maps the gimbal angles into the momentum space based on the types of CMGs involved and the geometry of the mounting configuration. This equation can be differentiated with respect to time in a spacecraft-fixed reference frame to yield

$$\tau = \dot{\boldsymbol{h}} = \omega \times \boldsymbol{h} + \boldsymbol{D}[\boldsymbol{h}_{\text{cmg}}(\boldsymbol{\theta})]\dot{\boldsymbol{\theta}} \tag{2}$$

where $\omega \in \boldsymbol{R}^3$ is the angular rate of the spacecraft in a spacecraft-fixed reference frame, $\boldsymbol{D}[\boldsymbol{h}_{\text{cmg}}(\boldsymbol{\theta})] \in \boldsymbol{R}^{3 \times m}$ denotes the derivative (Jacobian) of the mapping $\boldsymbol{h}_{\text{cmg}}(\boldsymbol{\theta})$, and $-\tau$ is the torque applied to the spacecraft due to the CMG gimbal motion. The torque is typically specified by an autopilot or a feedback control law.

In general, the number of degrees of freedom in the CMG system m is greater than the number required to provide three-axis control of the spacecraft. The problem that naturally arises is how to choose the gimbal rates $\dot{\boldsymbol{\theta}}$ to achieve a specified torque τ. This so-called steering problem is complicated by the inherent nonlinearity in these devices as well as the need to manage the redundancy in a CMG configuration to avoid geometric singularities. Singularities occur when the state of the CMG system is such that the output torque τ cannot be specified arbitrarily due to a drop in rank of the derivative in Eq. (2). The loss of rank corresponds to a loss of three-axis controllability of the spacecraft.

There have been a number of methods proposed for solving the CMG steering problem. Many of these methods are based on the idea of maximizing a configuration dependent objective function subject to the constraint that a specified torque is produced. The objective function is chosen such that its value reflects the desirability of a given configuration and is usually expressed as a function of the gimbal angles. In Ref. 1, the objective function used by the steering algorithm is the inverse of the *gain* of a double-gimballed CMG configuration. The gain is defined to be the product of the singular values of $\boldsymbol{D}[\boldsymbol{h}_{\text{cmg}}(\boldsymbol{\theta})]$, and singular configurations correspond to a gain of zero since they are associated with a drop in rank of this matrix. The gain function was considered in Ref. 2 and found to be ineffective for single gimbal devices due to the fact that it often cannot predict an impending singularity early enough to avoid it. In addition, it has been demonstrated that locally

Received Feb, 2, 1989; revision received May 30, 1989.

*Research Associate, Applied Research Laboratory, Systems Engineering Department.
†Section Chief, Flight Systems.
‡Member of Technical Staff, Sensor System Technology.
§Associate Professor, Department of Mechanical Engineering.
¶Professor and Head, Department of Mechanical Engineering.

optimal gain trajectories for single-gimballed CMGs can lead directly into singularities.[3] In Ref. 3, the authors use a table look-up to identify the configuration of globally optimal gain for each value of momentum for a specific mounting of four single-gimballed CMGs. This approach is not readily adaptable to configuration changes and requires onboard storage of a large data base.

To attain a margin of global effectiveness, other authors have investigated steering laws that either explicitly or implicitly locate singularities in the gimbal space and rotate the gimbal angles to avoid them. The steering laws proposed in Refs. 2, 4, and 5 steer the CMGs away from configurations that are known to be singular. The approach of Ref. 4 is to compute the sets of gimbal angles that are singular with respect to the requested torque vector and to rotate the gimbals to avoid them. In other words, gimbal angles are found for each CMG such that the CMG cannot instantaneously project momentum in the desired direction. The steering law then chooses rates that steer away from these gimbal states. The steering law in Ref. 5 exploits knowledge of a very specific mounting configuration to design an algorithm that implicitly avoids singularities.

The method of Ref. 2 is probably the most adaptable approach in that changes in hardware and CMG configuration are easily accommodated, and the objective function can be changed to reflect the most urgent of the CMG configuration priorities. In addition, the algorithm can be used to combine CMGs with jets to maintain vehicle control outside the torque envelope of the CMG system alone. Another advantage of this approach is that it explicitly incorporates limits on the maximum rates achievable by the gimbal drive motors. All other approaches that include this limitation incorporate it by scaling after a set of gimbal rates has been computed, thus preserving the direction chosen by the optimization but violating the requirement that a given torque be produced.

In Ref. 6, a number of algorithms are investigated for the control of single-gimballed CMGs. One of these methods is the "singularity" robust inverse method[7] which attempts to solve Eq. (2) by defining a vector consisting of the error in the torque produced by a choice of gimbal rates concatenated with the set of gimbal rates. A solution is found by minimizing a weighted Euclidean norm of this vector. Near singular states, this algorithm maintains reasonable gimbal rates by sacrificing torque in the direction associated with the singularity. Although the singularity robust inverse yields a steering algorithm that continues to function at singular states, the algorithm itself makes no effort to avoid these undesirable configurations.

Even though CMGs have been used in a number of applications, they have not found widespread use. Single-gimbal CMGs have been used on balloon-borne platforms[3] and in scissored pairs on early versions of NASA's Manned Maneuvering Unit, and have recently been installed on the Soviet Union's MIR space station.[8] Double-gimballed CMGs were used in NASA's Skylab[9] and are proposed for use on the planned NASA space station.[10] One of the principal difficulties in using CMGs for spacecraft attitude control is finding reliable solutions to the steering problem. One reason for this difficulty is that the steering problem does not consider the long-term behavior of the system but uses only the current state and torque request to compute gimbal rates. In other words, steering laws are local in nature and do not consider the effects of current decisions on the future. As a result, there is no steering law that can guarantee it will always keep the CMG configuration out of singular states. Single-gimballed CMG systems are particularly prone to lock up in singular configurations because of the reduced degrees of freedom.

A useful approach to CMG steering must provide a framework for exploiting redundancy to maintain CMG authority, behave in a sensible way near singular configurations, and be able to use the CMGs at their physical limitations when necessary. Though all steering algorithms attempt to redistribute individual rotors to more desirable configurations, Ref. 2 is the only published algorithm that treats gimbal limitations as a real constraint. With the exception of the singularity robust inverse method, which does not redistribute gimbal angles,[6] none of the published algorithms address the numerical difficulties that will occur near a singularity. This paper presents a general framework for the control of spacecraft with CMGs that considers each of the three requirements listed previously.

The approach presented in this paper is part of an investigation into applying the feedback linearization theory of Refs. 11 and 12 to the control of CMG-equipped spacecraft.[13] Feedback linearization theory has already been applied to several problems in spacecraft control. In Refs. 14 and 15, the theory is used to study optimal attitude maneuvers for torque-controlled spacecraft and spacecraft equipped with reaction wheels, respectively. Although the attitude control problems considered in both of these papers are quite similar, neither provides a realistic treatment when redundant actuators are included. In addition to the fact that redundancy is an important characteristic of CMG control systems, reaction wheel systems do not exhibit geometric singularities like CMG systems.

Applying the feedback linearization theory to a spacecraft model with CMGs, a transformation is obtained that simultaneously linearizes the dynamics of the spacecraft and decouples the redundant dynamics in the actuation system from the vehicle dynamics. This transformation is used to propose a class of steering algorithms in which a desired set of gimbal rates is computed, and then a normed approximation problem is solved to obtain a *best* match to the desired rates. This approximation problem is easily solved even when explicit bounds are included on the allowable gimbal results.

Using the approach to CMG steering developed here, the problem of designing a steering law is reduced to determining an algorithm for computing gimbal rates that move the CMG rotors toward desired configurations. This is conceptually simpler than the approach of determining a function whose derivative can be used to compute desired rates. Another advantage is that once a basic algorithm has been implemented, it is possible to add decision rules that can recognize and correct for known failure modes or to design an algorithm that is entirely rule based (i.e., an expert system). Skylab employed a "rule-based" system that relied on ground-based, manual intervention to resolve problems.[16] A modification to the basic algorithm that guarantees operation at and near singular states is presented in this paper.

In the following two sections a model for a CMG-equipped spacecraft is described, and a linearizing transformation is obtained. Because the spacecraft dynamics appear to be linear and independent of a subset of the CMGs, linear control laws can be applied to control the spacecraft attitude. Because the linearization obtained here is not an approximation, these control laws guarantee acceptable performance even for large rotations. A method for distributing gimbal rates among a group of CMG gimbals is then stated as a normed approximation problem requiring a set of desired gimbal rates that are to be matched. A particular algorithm is then proposed for computing the desired rates for double-gimballed CMGs. For the parallel-mounting configuration assumed in the NASA space station, two examples are presented in which published algorithms are known to fail. Note that because the geometric problem of singularity avoidance is considerably different for systems consisting of single-gimballed CMGs, the particular algorithm developed here for double-gimballed CMGs is not applicable to these devices; although the general approach remains valid. The attitude control problem and momentum management are not discussed in this paper; these issues have been addressed in Ref. 13 and in a forthcoming paper.

Model Derivation for a Control Moment Gyroscope-Equipped Spacecraft

In this section, a mathematical model is developed for a CMG-equipped spacecraft. The vehicle attitude is represented by a quaternion, and a differential equation is derived that characterizes its evolution. It will be shown in the following section that the attitude variable to be controlled can be chosen arbitrarily once a specific vehicle model is defined. A kinematical model for a double gimbal CMG is presented and incorporated into a model of a rigid spacecraft rotating in an inertial reference frame.

Let A and B denote a pair of right-handed reference frames, and assume that B has been rotated with respect to A through an angle θ about an axis defined by the unit vector $\hat{\boldsymbol{u}}$ expressed in the basis A. The quaternion of reference frame B with respect to A is defined to be the ordered quadruple

$$\boldsymbol{q}_A^B = \begin{Bmatrix} \bar{q}_0 \\ \bar{\boldsymbol{q}} \end{Bmatrix} = \begin{Bmatrix} q_0 \\ q_1 \\ q_2 \\ q_3 \end{Bmatrix} = \begin{Bmatrix} \cos(\theta/2) \\ \hat{\boldsymbol{u}} \sin(\theta/2) \end{Bmatrix} \in R^4 \tag{3}$$

This definition is more restrictive than encountered in mathematical discussions[17] but is sufficient for the purposes here. Quaternion multiplication is defined as

$$\boldsymbol{pq} = \begin{bmatrix} p_0 q_0 - \bar{\boldsymbol{p}}^* \bar{\boldsymbol{q}} \\ p_0 \bar{\boldsymbol{q}} + p_0 \bar{\boldsymbol{q}} + \bar{\boldsymbol{p}} \times \bar{\boldsymbol{q}} \end{bmatrix} = \begin{bmatrix} p_0 & -p_1 & -p_2 & -p_3 \\ p_1 & p_0 & -p_3 & p_2 \\ p_2 & p_3 & p_0 & -p_1 \\ p_3 & -p_2 & p_1 & p_0 \end{bmatrix} \begin{bmatrix} q_0 \\ q_1 \\ q_2 \\ q_3 \end{bmatrix} \tag{4}$$

where * and $\times$ denote the ordinary vector dot and cross products, respectively. The conjugate, $\boldsymbol{q}^*$ of a quaternion $\boldsymbol{q}$ is defined by

$$\boldsymbol{q}^* = \begin{Bmatrix} q_0 \\ -\bar{\boldsymbol{q}} \end{Bmatrix} = \begin{Bmatrix} q_0 \\ -q_1 \\ -q_2 \\ -q_3 \end{Bmatrix} \tag{5}$$

Throughout this paper, it will be necessary to compute quaternion products of only two types of quaternions: quaternions associated with rotations of orthogonal reference frames [Eq. (3)], and quaternions associated with vector-valued quantities in $\boldsymbol{R}^3$. In this paper, the symbol $\boldsymbol{q}$ is reserved exclusively for quaternions that represent rotations as defined by Eq. (3); superscripts and subscripts are added to distinguish such quaternions from one another and to denote the elements of a quaternion. In the derivation that follows, equations are presented that include products of quaternions with physical quantities such as momentum and angular rate. These physical quantities are represented by quaternions whose scalar part is zero, and the products are computed according to the rules of quaternion multiplication [Eq. (4)]. For clarity, the notation $\{0/x\}$ is used to emphasize when a three-dimensional quantity x is to be treated as a quaternion in a multiplication.

Note that a consequence of the definition of Eq. (3) is that quaternions that characterize rotations of orthogonal reference frames have a Euclidean norm of one; given any three elements of such a quaternion, it is possible to compute the fourth. In particular, the expression

$$q_0 = \sqrt{1 - \sum_{i=1}^{3} q_i^2} \tag{6}$$

can be used to compute the scalar part of a quaternion from its vector part. As a result, all the quaternions that are considered here are uniquely determined by their last three components; the scalar part is either zero or given by Eq. (6). From now on, it will be assumed that all quaternions are represented by elements of $\boldsymbol{R}^3$; consequently, the definition of quaternion multiplication must be modified to use either zero or Eq. (6) when the scalar part of the quaternion is needed. Although this assumption may seem unnecessary, it is justified for the following reason. When deriving the linearizing transformations in the next section, it is necessary to compute the derivative of a function of a quaternion with respect to an element of the quaternion. Because of the constraint implicit in Eq. (3), care must be taken when evaluating this derivative because $\partial \boldsymbol{q}_i / \partial \boldsymbol{q}_j \neq 0$ for $i, j \in [0, \ldots, 3]$. By formally substituting Eq. (6) for $\boldsymbol{q}_0$ when it appears, it can be assumed that the derivative $\partial \boldsymbol{q}_i / \partial \boldsymbol{q}_j = 0$ for $i \neq j$. This simplifies the notation of the following section and clarifies for the reader the computations involved. Note that the previously defined notation for quaternion arithmetic is not changed in this or the next section. The reader should regard the modification to conventional quaternion algebra as purely computational; the meanings of the expressions are unchanged.

In the following sections, it will be necessary to compute the time rate of change of a quaternion due to the relative rotation of two reference frames. For example, if the quaternion transforms vectors in inertial coordinates into a spacecraft fixed frame, the quaternion will change with time as the spacecraft rotates. The time derivative of a quaternion $\boldsymbol{q}_A^B$ is computed assuming reference frame B is rotating at a relative angular rate ω^B, which has been coordinatized in the reference frame B. It can be shown that

$$\dot{\boldsymbol{q}}_A^B = \frac{1}{2} \begin{Bmatrix} 0 \\ \omega^B \end{Bmatrix} \boldsymbol{q}_A^B = \frac{1}{2} \begin{bmatrix} q_1 & \sqrt{1 - q_1^2 - q_2^2 - q_3^2} & -q_3 & q_2 \\ q_2 & q_3 & \sqrt{1 - q_1^2 - q_2^2 - q_3^2} & -q_1 \\ q_3 & -q_2 & q_1 & \sqrt{1 - q_1^2 - q_2^2 - q_3^2} \end{bmatrix} \begin{bmatrix} q_1 \\ q_2 \\ q_3 \end{bmatrix} \tag{7}$$

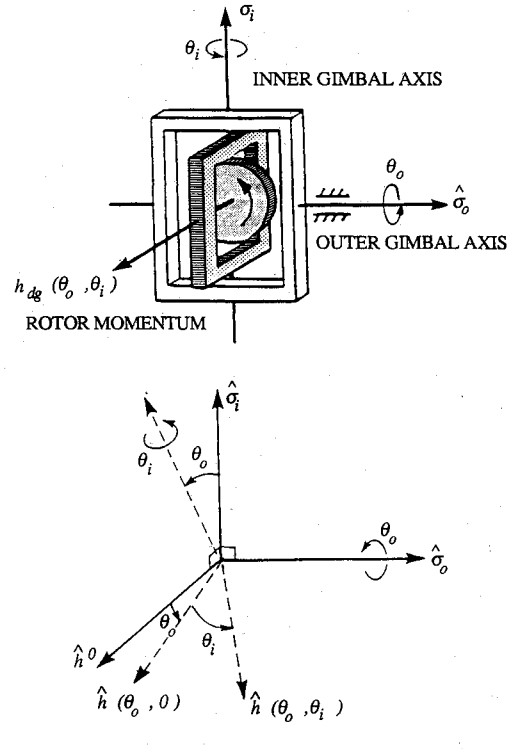

Fig. 1 Schematic drawing and reference frame for a double-gimballed CMG.

Note that the quaternion product has been expanded here to illustrate how the modification discussed in the previous paragraph affects the computations.

To derive dynamical equations for a spacecraft equipped with CMGs, it is necessary to have a kinematical model for CMGs. Figure 1 shows a schematic of a double-gimballed CMG. In this figure $\hat{\boldsymbol{\sigma}}_o$ is a unit vector along the outer gimbal axis. This axis is fixed with respect to the spacecraft. The unit vector $\hat{\boldsymbol{\sigma}}_i$ lies along the reference inner gimbal axis corresponding to $\theta_o = 0$, and the third vector in the triad is defined to be orthogonal to $\hat{\boldsymbol{\sigma}}_o$ and $\hat{\boldsymbol{\sigma}}_i$ (i.e., $\hat{\boldsymbol{h}}^0 = \hat{\boldsymbol{h}}(\theta_o = 0, \theta_i = 0) = \hat{\boldsymbol{\sigma}}_o \times \hat{\boldsymbol{\sigma}}_i$). The CMG momentum vector can be expressed in the basis $(\hat{\boldsymbol{\sigma}}_o, \hat{\boldsymbol{\sigma}}_i, \hat{\boldsymbol{h}}^0)$ defined relative to a spacecraft fixed frame. Allowing h_{mag} to denote the magnitude of the rotor momentum, the expression

$$\boldsymbol{h}_{\text{dg}}(\theta_o, \theta_i) = \boldsymbol{h}_{\text{mag}}[(\hat{\boldsymbol{h}}^0 \cos\theta_o - \hat{\boldsymbol{\sigma}}_i \sin\theta_o)\cos\theta_i + \hat{\boldsymbol{\sigma}}_o \sin\theta_i] \quad (8)$$

characterizes the momentum vector of a double-gimballed CMG as a function of (θ_o, θ_i), the outer and inner gimbal angles, respectively.

Equation (8) expresses the momentum vector of a CMG in a spacecraft-fixed reference frame. In general, the momentum vectors of a group of CMGs will be expressed in a common frame. Given a group of CMGs, Eq. (8) can be used to express the net momentum of the CMG system in a spacecraft-fixed reference frame as a sum over the set of CMGs

$$\boldsymbol{h}_{\text{cmg}}(\boldsymbol{\theta}) = \sum_{k=1}^{N_{\text{cmg}}} \boldsymbol{h}_{\text{dg}}^k(\theta_o, \theta_i) \quad (9)$$

where $\boldsymbol{h}_{\text{dg}}^k \in R^3$ is the momentum of the kth CMG, and $\boldsymbol{\theta} \in R^m$ denotes the set of gimbal angles.

The attitude of the spacecraft is characterized by a quaternion $\boldsymbol{q}$, which defines the relative orientation of a spacecraft-fixed reference frame, denoted B, with respect to an inertial frame (since this will be the only quaternion used, subscripts and superscripts are not needed). It is assumed here that the total angular momentum of the spacecraft in inertial coordinates $\boldsymbol{h}^I$ is known or can be computed. The total momentum can be computed in body-fixed coordinates from knowledge of the spacecraft angular rate and the CMG configuration. In many configurations, the momentum in inertial coordinates is reasonably constant for long periods of time. The momentum vector $\boldsymbol{h}^I$ can be transformed into the basis of the spacecraft-fixed frame by the quaternion product

$$\boldsymbol{h}^B = \boldsymbol{q}^* \boldsymbol{h}^I \boldsymbol{q} \quad (10)$$

The momentum in the spacecraft reference frame $\boldsymbol{h}^B$ can be expressed as

$$\boldsymbol{h}^B = \boldsymbol{h}_{\text{cmg}}(\boldsymbol{\theta}) + \boldsymbol{h}_{\text{spacecraft}} = \boldsymbol{h}_{\text{cmg}}(\boldsymbol{\theta}) + I\omega^B \quad (11)$$

where $\omega^B \in \boldsymbol{R}^3$ denotes the spacecraft's angular rate, and $I \in \boldsymbol{R}^{3\times 3}$ denotes the inertia matrix of the vehicle. Both $\boldsymbol{h}_{\text{cmg}}(\boldsymbol{\theta})$, and ω^B are expressed in the body-fixed coordinate frame B. The angular rate of the spacecraft can be determined from the total momentum and the momentum stored in the CMGs by solving eq. (11) for ω^B

$$\omega^B = I^{-1}[\boldsymbol{h}^B - \boldsymbol{h}_{\text{cmg}}(\boldsymbol{\theta})] = I^{-1}[\boldsymbol{q}^* \boldsymbol{h}^I \boldsymbol{q} - \boldsymbol{h}_{\text{cmg}}(\boldsymbol{\theta})] \quad (12)$$

This expression can be substituted into Eq. (7) to obtain an expression for the derivative of the attitude quaternion in terms of the constant inertia matrix, the known inertial angular momentum, and the attitude quaternion of the spacecraft.

$$\dot{\boldsymbol{q}} = \frac{1}{2}\begin{Bmatrix} 0 \\ I^{-1}[\boldsymbol{q}^* \boldsymbol{h}^I \boldsymbol{q} - \boldsymbol{h}_{\text{cmg}}(\boldsymbol{\theta})] \end{Bmatrix} \boldsymbol{q} \quad (13)$$

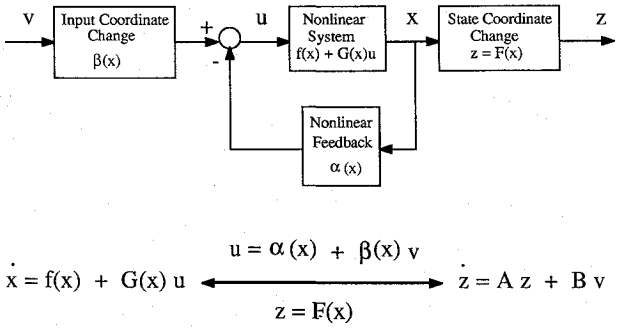

Fig. 2 Implementation of a linearizing feedback transformation.

Note that the preceding expression could have been written with momentum expressed in body coordinates [Eq. (11)]. If it is desired to include variations in momentum, the transformation computed in the next section requires knowledge of the net rate of momentum change. Since neglecting momentum changes is equivalent to neglecting external torques, the assumptions made here are identical to those of other published steering algorithms.

To complete the derivation of the equations for rotation in the absence of external torques, it is necessary to consider the control or input variable. CMG steering algorithms usually choose the set of gimbal rates as the control variable. The equations that describe the evolution of the gimbal angles are

$$\dot{\boldsymbol{\theta}} = \boldsymbol{u} \quad (14)$$

where $\boldsymbol{\theta}, \boldsymbol{u} \in \boldsymbol{R}^m$. Under the stated assumptions, the dynamics of the combined spacecraft/CMG system are described by the state equations (13) and (14). These equations describe the attitude dynamics and the evolution of the gimbal angles, respectively.

The gimbal rate equation (14) is also useful when it is desirable to include physical limits on the individual gimbal drives. In some circumstances, it may be more realistic to consider torque limits on the gimbal-drive motors, especially when double-gimbal CMGs are being used. With double-gimbal CMGs, motion of one gimbal can produce a torque along the axis of the other. The need to back drive the gimbals can impose restrictions that cannot be accounted for without developing a higher-order model. In this discussion, it is assumed that the gimbal rates—as expressed in the individual CMG frames—can be commanded as the control variables. This assumption is consistent with conventional operation and does not result from a limitation imposed by the feedback linearization theory that will be applied in the next section. It may be desirable in future efforts to examine the effects resulting from including the dynamics of the gimbal drive motors in the model.

Feedback Linearization of the Spacecraft Model

The basic idea behind feedback linearization[11, 12] is illustrated in Fig. 2. Given a nonlinear system of equations of the form

$$\dot{\boldsymbol{x}} = f(\boldsymbol{x}) + \sum_{i=1}^{m} g_i(\boldsymbol{x})u_i = f(\boldsymbol{x}) + G(\boldsymbol{x})\boldsymbol{u} \quad (15)$$

the objective is to obtain a nonlinear change of coordinates in the state $F(\boldsymbol{x})$, a nonlinear feedback $\alpha(\boldsymbol{x})$, and a linear, invertible change of coordinates in the input $\beta(\boldsymbol{x})$ such that the input/output behavior of the sytem illustrated in Fig. 2 has a prescribed linear form. Note that this type of linearization is not an approximation, but an exact transformation in which the linear model can be made to have a particularly simple form. Another feature of the transformation shown in this figure is that it is applied externally to the system equations;

the transformation does not require internal modifications to a given model [Eq. (15)]. As a consequence, the feedback transformations employed here are, in principle, implementable in hardware and software.

For the system of interest in this paper, Eqs. (13) and (14), the results of Ref. 11 can be used to show that there exists a memoryless, nonlinear state transformation $z = F(q, \theta)$ and an input transformation $u = \alpha(q, \theta) + \beta(q, \theta)v$, such that the evolution of the transformed system is described by linear constant coefficient differential equations of the form

$$\dot{z} = Az + Bv \tag{16}$$

Furthermore, the state and control vectors of the linearized system can be partitioned into the forms $z = (z_1^T, z_2^T, z_3^T)^T$ and $v = (v_1^T, v_2^T)^T$, respectively, with $z_1 \in R^3$, $\dot{z}_1 = z_2$, $\dot{z}_2 = v_1$ and $\dot{z}_3 = v_2 \in R^{m-3}$. These definitions imply that the matrices (A, B) must have the special forms

$$A = \left[\begin{array}{c|c|c} 0 & I_3 & 0 \\ 0 & 0 & 0 \\ \hline 0 & 0 & 0 \end{array}\right], \qquad B = \left[\begin{array}{c|c} 0 & 0 \\ I_3 & 0 \\ \hline 0 & I_{m-3} \end{array}\right] \tag{17}$$

This assumption regarding the structure of the pair (A, B) can be made without loss of generality, since all achievable linear behaviors can be obtained by applying linear feedback, linear input transformations, and linear state transformations to the system defined by Eqs. (16) and (17).[18] In other words, the forms of Eq. (17) were chosen to simplify the problem of obtaining the linearizing tranformations; once the system is made to behave like Eq. (16), a separate design procedure will yield a control sytem that yields desired characteristics.

A simple justification for the form of the matrices (17) is as follows. The linear system defined by Eqs. (16) and (17) contains three sets of independent double integrators. These second-order subsystems are related to the second-order rotational dynamics of the spacecraft, and the input variable v_1 is related to the spacecraft acceleration. Since the state components z_3 evolve independently of the spacecraft attitude, trajectories of the variables z_3 can be interpreted as null-motions of the CMG gimbals. In other words, these states are associated with the redundant degrees of freedom in the CMG system.

Once computed, the feedback transformation simplifies the original system equations in two important ways. First, the nonlinear spacecraft equations are transformed to a very simple linear form; familiar techniques from linear systems theory can then be applied to derive control laws for the spacecraft. Second, the linearized system of equations contains state variables that are explicitly related to the available freedom in the choice of gimbal trajectories. In the sequel, it will be shown how to construct the state and input transformations from a particular choice of z_1 and z_3 for which the transformations are known to exist.

In this paper, the (three) elements of the attitude quaternion are chosen for the elements of z_1. The advantage of redefining quaternion arithmetic becomes apparent when expanding the equations that follow. Even though quaternions have been chosen to represent attitude in the model equations here, there may be practical reasons for choosing one or more Euler angles to be directly controlled. Whatever attitude variables are chosen for z_1, the transformation derived here will linearize and decouple their dynamics. Once the variables z_1 are chosen, the functional relationship between the chosen attitude variables and the attitude quaternion must be obtained. The relationship can be expressed symbolically as

$$z_1 = F_1(q) \left[= \begin{bmatrix} 1 & 0 & 0 \\ 0 & 1 & 0 \\ 0 & 0 & 1 \end{bmatrix} \begin{bmatrix} q_1 \\ q_2 \\ q_3 \end{bmatrix} \right] \tag{18}$$

where the term in brackets has been used in the approach presented here. This expression can be differentiated to obtain the value of z_2 in terms of the state variables (q, θ)

$$z_2 = \dot{z}_1 = [D_q F_1(q)]\dot{q} = F_2(q, \theta)[= \dot{q}] \tag{19}$$

where Eq. (13) is substituted to eliminate $\dot{q}$. The notation $[D_q F(q)]$ has been introduced to denote the derivative of a vector valued function F with respect to a vector variable q. The ith column of the derivative matrix consists of the partial derivatives of the elements of $F(q)$ with respect to the scalar variable q_i. The functional form of Eq. (18) has been maintained throughout the discussion to enable interested readers to formulate the approach described here for any choice of attitude control variables and to emphasize that the approach is not inherently based on quaternions.

Although a more general choice is possible, z_3 will be chosen as follows. Assuming that the CMG configuration is not singular, it is possible to order the gimbal angles of the vector θ such that the rank of the 3×3 matrix

$$A_1(\theta) = [D_{\theta_1} h_{\text{cmg}}(\theta), D_{\theta_2} h_{\text{cmg}}(\theta), D_{\theta_3} h_{\text{cmg}}(\theta)] = D_\phi h_{\text{cmg}}(\theta) \tag{20}$$

is three. Here the symbol $\phi = [\theta_1, \theta_2, \theta_3]^T$ has been used to denote the vector consisting of the first three elements of the ordered gimbal angle vector. Nonsingularity of this matrix implies that the torques produced by the three gimbal rates $[u_1, u_2, u_3]$ span three space. The component of the linearized state variable represented by z_3 is defined to be

$$z_3 = \begin{bmatrix} \theta_4 \\ \vdots \\ \theta_m \end{bmatrix} \tag{21}$$

This completes construction of the coordinate tranformation $F(x) = [z_1^T, z_2^T, z_3^T]^T$ that maps the state variables of the model, $x = (q, \theta)$, to those of the linearized system.

It now remains to construct the feedback and input transformation. By assumption, the control variable v has the interpretation

$$v = \begin{bmatrix} v_1 \\ v_2 \end{bmatrix} = \begin{bmatrix} \ddot{z}_1 \\ \dot{z}_3 \end{bmatrix} = \frac{d}{dt} \begin{bmatrix} z_2 \\ z_3 \end{bmatrix} \tag{22}$$

This expression can be evaluated by substituting Eq. (19) and (21) and then differentiating to yield

$$v = \begin{bmatrix} [D_q F_2] & [D_\theta F_2] \\ 0 & [0 \quad I_{m-3}] \end{bmatrix} \begin{bmatrix} \dot{q} \\ \dot{\theta} \end{bmatrix} = \begin{bmatrix} [D_q F_2] \\ 0 \end{bmatrix} \dot{q} + \begin{bmatrix} [D_\phi F_2] & [D_{z_3} F_2] \\ 0 & I_{m-3} \end{bmatrix} \dot{\theta} \tag{23}$$

Once again noting that the $\dot{q}$ is a function of (q, θ) and using the fact that $\dot{\theta} = u$, the previous equation can be written in the form

$$v = w(q, \theta) + A(q, \theta)u \tag{24}$$

Note that if the matrix $A(q, \theta)$ is invertible, then Eq. (24) can be solved to yield an input transformation of the required form

$$u = [A(q, \theta)]^{-1} w(q, \theta) + [A(q, \theta)]^{-1} v = \alpha(q, \theta) + \beta(q, \theta)v \tag{25}$$

or equivalently,

$$u = \begin{bmatrix} \alpha_1 \\ 0 \end{bmatrix} + [\beta_1 \beta_2] \begin{bmatrix} v_1 \\ v_2 \end{bmatrix} \tag{26}$$

Necessary and sufficient conditions for Eq. (24) to be solvable for $\boldsymbol{u}$ are that the function F_1 in Eq. (18) be invertible and the matrix A_1 in Eq. (20) be nonsingular. From Eq. (23), it is clear that the matrix $A(\boldsymbol{q}, \boldsymbol{\theta})$ will be invertible if the 3×3 submatrix in the upper left corner is nonsingular. This matrix is given by

$$\begin{aligned} \boldsymbol{D}_\phi \boldsymbol{F}_2(\boldsymbol{q}, \boldsymbol{\theta}) &= [\boldsymbol{D}_q \boldsymbol{F}_1(\boldsymbol{q})][\boldsymbol{D}_\phi \dot{\boldsymbol{q}}] \\ &= -\frac{1}{2}[\boldsymbol{D}_q \boldsymbol{F}_1(\boldsymbol{q})]\left[\boldsymbol{D}_\phi\left[\begin{Bmatrix} 0 \\ \boldsymbol{h}_{\text{cmg}} \end{Bmatrix}\boldsymbol{q}\right]\right] \end{aligned} \tag{27}$$

By the inverse function theorem, invertibility of F_1 implies nonsingularity of the matrix $\boldsymbol{D}_q \boldsymbol{F}_1(\boldsymbol{q})$; therefore, it only remains to show that the remaining 3×3 matrix is nonsingular. Observing that

$$\boldsymbol{D}_\phi\left[\begin{Bmatrix} 0 \\ \boldsymbol{h}_{\text{cmg}} \end{Bmatrix}\boldsymbol{q}\right] = \boldsymbol{D}_\phi\left[\begin{bmatrix} \boldsymbol{h}^1_{\text{cmg}} & 0 & -\boldsymbol{h}^3_{\text{cmg}} & \boldsymbol{h}^2_{\text{cmg}} \\ \boldsymbol{h}^2_{\text{cmg}} & \boldsymbol{h}^3_{\text{cmg}} & 0 & -\boldsymbol{h}^1_{\text{cmg}} \\ \boldsymbol{h}^3_{\text{cmg}} & -\boldsymbol{h}^2_{\text{cmg}} & \boldsymbol{h}^1_{\text{cmg}} & 0 \end{bmatrix}\begin{bmatrix} \sqrt{1-\boldsymbol{q}_1^2-\boldsymbol{q}_2^2-\boldsymbol{q}_3^2} \\ \boldsymbol{q}_1 \\ \boldsymbol{q}_2 \\ \boldsymbol{q}_3 \end{bmatrix}\right] \tag{28}$$

it can be seen that the rows of the preceding matrix consist of linear combinations of the rows of the matrix A_1 in Eq. (20). Because Eq. (28) implies that one of the coefficients in each linear combination must differ in sign from the corresponding coefficient in the other two combinations, each row of the matrix (28) must be a unique combination of the rows of A_1. The converse follows immediately: singularity of $\boldsymbol{D}_\phi \dot{\boldsymbol{q}}$ implies singularity of Eq. (20), and singularity of $\boldsymbol{D}_q \boldsymbol{F}_1(\boldsymbol{q})$ implies that $F_1(\boldsymbol{q})$ is not invertible.

In concluding this section, it is useful to discuss the implications when one of the necessary and sufficient conditions fails. Singularity of $\boldsymbol{D}_\phi \dot{\boldsymbol{q}}$ implies that the CMG configuration is singular, since singularity of A_1 implies that there is a direction in which the CMG system cannot instantaneously project momentum. A later section presents a method for dealing with this eventuality. Noninvertibility of $F_1(\boldsymbol{q})$ implies that it is not possible to associate a unique physical orientation of the body with the parameters z_1. This difficulty arises due to the choice of attitude variables and is not a limitation of the methodology developed here; any attitude control law employing these parameters will have to deal with these singularities. In practice, this presents no difficulty since the singularity can be eliminated by merely changing the reference attitude for which the attitude variables are defined.

Gimbal Rate Distribution by Normed Approximation

In this section, an approach to distributing control effort among a group of CMGs is developed that employs the linearizing transformation developed previously. Although the dynamics of the system to be controlled have been made linear by the transformation of Eq. (25), the steering problem has not been solved. Effectively, the linearizing transformation decouples the problem of spacecraft attitude control, and the problem of distributing control effort among the available actuators has not been addressed. If it were not for the kinematic redundancy in the CMG system, the solution to the linearization problem would be adequate and unique; no steering problem would exist.

A natural choice of gimbal rates would be one that requires a minimal effort to produce a desired influence on the spacecraft. This would be sufficient if there were no dynamics associated with the CMGs. In the problem at hand, there are certain configurations or CMG states that are to be avoided. Consequently, there may be a desired value u_d for the gimbal rates. The problem of computing gimbal rates u that are close to the desired value can be stated as a normed approximation problem

$$\min_u \|u_d - u\| \tag{29}$$

subject to the constraint that a specified acceleration be produced. Note that the feedback part of the linearizing transformation [Eq. (25)] yields an affine parameterization of all gimbal rates that produce a specified attitude acceleration. Once the first three elements of the control vector of the linear system have been fixed, the remaining elements can be selected arbitrarily without changing the commanded acceleration. The parameterization effectively eliminates the torque constraint associated with the steering problem and reduces the number of variables that need to be considered by three. Assuming that the component v_1 of the linearized control vector (equivalently, the commanded torque) is specified and can be regarded as fixed, substitution of Eq. (26) into Eq. (29) yields

$$\min_{v_2} \|a - \beta_2 v_2\| \tag{30}$$

where $a = u_d - \alpha - \beta_1 v_1$. From a practical point of view, it is useful to impose limits on the individual inputs of the form

$$-u_p^i \le u_i \le u_p^i \tag{31}$$

where u_p^i is the maximum gimbal rate associated with gimbal i. Fast numerical methods exist for solving Eq. (30) with constraints (31) in three important norms: the 1-norm defined by

$$\|\boldsymbol{x}\|_1 = \sum_{i=1}^{n} |x_i| \tag{32}$$

the 2 norm (the usual Euclidean norm) defined by

$$\|\boldsymbol{x}\|_2 = \left\{\sum_{i=1}^{n} |x_i|^2\right\}^{1/2} \tag{33}$$

and the ∞ norm defined by

$$\|\boldsymbol{x}\|_\infty = \max_i |x_i| \tag{34}$$

The constrained problem in the 2 norm can be formulated directly as a quadratic programming problem.[19] The 1- and ∞-norm problems can be formulated as linear programs as shown in Refs. 20 and 21, respectively.

Algorithm for Computing Desired Rates for Double-Gimbal Control Moment Gyroscopes

In the following paragraphs, an algorithm for computing a desired set of gimbal rates for a group of double-gimballed CMGs is developed. The algorithm is based on computing a desired rotation vector for each CMG. The direction and magnitude of the rotation vector of a CMG rotor correspond to the axis and rate of rotation, respectively, of the rotor due to gimbal motion. The rotation vectors are chosen to move the CMG rotors to maximize the amount of momentum that can be projected instantaneously in any direction, to avoid line up with the commanded torque vector, and to keep inner gimbal angles small. The desired rotation vector for a CMG is computed as the sum of a set of rotation vectors, each of

which individually attempts to achieve one of these objectives. From the desired rotation vector, desired gimbal rates are derived for each CMG. This section concludes with a brief explanation of how the proposed steering law is incorporated into an attitude control system.

One method for maintaining good three-axis controllability with double-gimballed CMGs is to keep the mutual angles between rotors as large as possible. Should a torque be commanded along a direction aligned with a CMG momentum vector, this will insure that all of the other CMGs can contribute to producing the torque. Since singular states of double-gimballed CMG systems are always associated with a mutual alignment of rotors, this is also equivalent to avoiding singularities. For each CMG, the term that achieves this in the rotation vector computation is

$$\boldsymbol{\sigma}_1^k = \sum_{j \neq k} \frac{u_p}{\pi} [\cos^{-1}(\hat{\boldsymbol{h}}^k \cdot \hat{\boldsymbol{h}}^j) - \pi] \text{unit}(\hat{\boldsymbol{h}}^k \times \hat{\boldsymbol{h}}^j) \tag{35}$$

where u_p denotes the peak gimbal rate, $\hat{\boldsymbol{h}}^k$ denotes a unit vector along rotor axis k, and the cross product is normalized to have unit norm. The rotation vector $\boldsymbol{\sigma}_1^k$ can be interpreted as a desired angular velocity for the kth CMG rotor; the subscript indicates that it is the first term in a sum of such vectors. Rotating each CMG in this way will move the rotors to a configuration in which they are distributed symmetrically about the total CMG momentum vector. The inverse cosine term represents the angle between individual momentum vectors.

If a rotor is allowed to align with the commanded torque direction, the corresponding CMG cannot generate torque along the commanded axis. The term that steers rotors away from such configurations is

$$\boldsymbol{\sigma}_2^k = \begin{cases} 0 & \text{if } \cos^{-1}(\hat{\boldsymbol{h}}^k \cdot \hat{\boldsymbol{\tau}}) \geq k^\tau \\ \sum_{k=1}^{m} \frac{u_p}{k^\tau} [\cos^{-1}(\hat{\boldsymbol{h}}^k \cdot \hat{\boldsymbol{\tau}}) - k^\tau] \text{unit}(\hat{\boldsymbol{h}}^k \times \hat{\boldsymbol{\tau}}) & \text{if } \cos^{-1}(\hat{\boldsymbol{h}}^k \cdot \hat{\boldsymbol{\tau}}) < k^\tau \end{cases} \tag{36}$$

where $\hat{\boldsymbol{\tau}}$ denotes a unit vector in the direction of the requested torque; k^τ represents the largest angle between the momentum and torque vectors for which this term contributes and is an input to the algorithm. The cross product is normalized as before. To avoid numerical difficulties, an arbitrary gimbal axis is used in the neighborhood of an exact line up of vectors in Eqs. (35) and (36).

To simplify notation in defining the next two contributions to the rotation vector, a piecewise linear function Φ is defined by

$$\Phi(a, b, c, d) = \begin{cases} 0 & \text{if } \left|\frac{a}{b}\right| \leq c \\ \frac{a}{|a|} \frac{|a/b| - c}{d - c} & \text{if } c < \left|\frac{a}{b}\right| \leq d \\ 1 & \text{if } \left|\frac{a}{b}\right| > d \end{cases} \tag{37}$$

where (a, b, c, d) are constants with $|a| \leq b$, and $0 \leq c < d \leq b$.

It is desirable to keep the inner gimbal angles small, both to avoid potential hardware stops, and because the torque due to the outer gimbal rate is proportional to the cosine of the inner gimbal angle. A rotation vector which reduces the inner gimbal displacements is

$$\boldsymbol{\sigma}_3^k = -u_p \Phi(\theta_i^k, \theta_{\text{stop}}, k_1^{\text{inner}}, k_2^{\text{inner}}) \hat{\boldsymbol{\sigma}}_i^k \tag{38}$$

where θ_i^k denotes the inner gimbal displacement of CMG k, θ_{stop} is the displacement to a gimbal stop, k_1^{inner}, k_2^{inner} are constants, and $\hat{\boldsymbol{\sigma}}_i^k$ is the unit vector along the inner gimbal axis of the kth CMG.

In studying several maneuvers, it was found necessary to include a term in the calculation of the desired rotation vector, which would rotate the outer gimbal angle if the inner gimbal was being forced against a stop. Associated with each CMG is the rotation rate

$$\boldsymbol{\sigma}_4^k = \pm u_p \Phi(\theta_i^k, \theta_{\text{stop}}, k_1^{\text{outer}}, k_2^{\text{outer}}) \hat{\boldsymbol{\sigma}}_o^k \tag{39}$$

where θ_i and θ_{stop} are as before, k_1^{outer}, k_2^{outer} are constants, and $\hat{\boldsymbol{\sigma}}_o^k$ is a unit vector along the outer gimbal axis of the kth CMG. The initial sign of this rotation is chosen to move the rotor away from the inner gimbal rotation plane and is not changed until $\boldsymbol{\sigma}_4^k$ is set to zero. The need for such a term will be explained in connection with one of the examples.

For each CMG, the desired rotation vector is found by taking a weighted combination of the four rotation vectors previously defined.

$$\boldsymbol{\sigma}_d^k = \sum_{j=1}^{N_{\text{cmg}}} k_j \boldsymbol{\sigma}_j^k \tag{40}$$

From this composite rotation vector, it is possible to compute a unique set of gimbal rate commands that produce the desired rotor motion for the given CMG by solving the linear equation

$$\boldsymbol{\sigma}_d^k \times \hat{\boldsymbol{h}}^k = a(\hat{\boldsymbol{\sigma}}_i^k \times \hat{\boldsymbol{h}}^k) + b(\hat{\boldsymbol{\sigma}}_o^k \times \hat{\boldsymbol{h}}^k) \tag{41}$$

for the scalars a and b, which represent the desired inner and outer gimbal rates, respectively, for the kth CMG. Proceeding in this way for each CMG, a vector of desired gimbal rates, $u_d \in \boldsymbol{R}^m$ is computed, and the normed approximation strategies of the previous section can be used to calculate actual gimbal rates based on these desired rates. In the following section, an implementation of a steering law based on this desired rate computation and the approximation algorithms is described.

Implementation of the Proposed Algorithm

In this section, an algorithm that implements a CMG steering law based on normed approximation and the desired rate computation of the previous section is described. The program has been implemented in FORTRAN on a VAX® computer along with a rigid-body simulation of a spacecraft. A flow chart of the steering algorithm is shown in Fig. 3. The inputs are the current CMG gimbal angles, spacecraft attitude quaternion, derivative of the quaternion, and second derivative of the quaternion, which is determined by an autopilot or control law. The second derivative of the quaternion could be computed based on linear feedback of the state variables z_1 and z_2 (Ref. 14) or on direct quaternion feedback.[22] If the autopilot or control law has been designed to command the steering algorithm with a torque or acceleration, $\ddot{\boldsymbol{q}}$ can be determined from the derivative of Eq. (7). Since quaternions are algebraically related to any set of attitude variables, there is no loss of generality by assuming the quaternion acceleration is the input.

The steering algorithm first tests the CMG gimbal angles to see if the CMG configuration is near a singular state. If the gain function is above a certain threshold, a routine that monitors the transformation is called. The routine MONITOR checks that the three gimbal rates that do not appear in the linearized control vector are capable of producing torques in all directions. Their ability to control the spacecraft is deter-

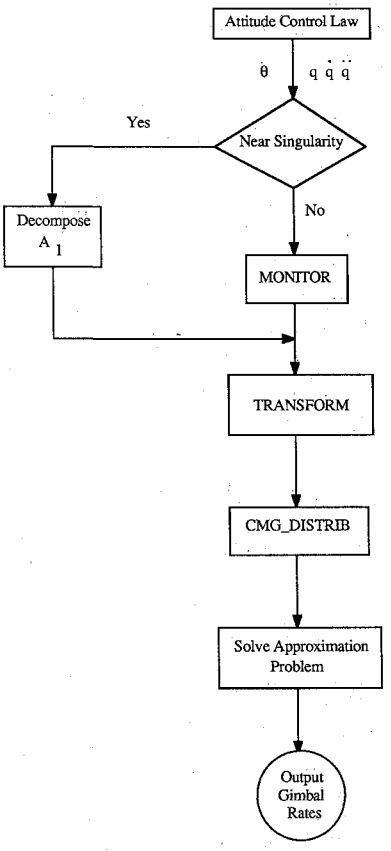

Fig. 3 Flow chart of CMG steering algorithm.

mined by the determinant of the matrix formed by the three columns of the matrix (20). If the determinant is below a certain threshold, a new combination of three gimbal angles is found that produces the largest determinant, and these three gimbal rates will not appear in the transformed control. Note that this effectively amounts to reindexing the gimbal rates. These changes occur internally to the tranformation illustrated in Fig. 2 and are transparent to both the attitude control functions and the normed approximation algorithm.

If the CMG rotors are near a singular configuration, then there will be no combination of three CMGs that can produce torques adequately in all directions. Most steering algorithms do not consider this situation at all, even though most steering algorithms attempt some sort of singularity avoidance. The most common symptom of such a failure is termed gimbal lock, which occurs when the CMGs become stuck in a singular configuration, possibly due to numerical errors or because the steering algorithm is attempting to normalize gimbal rates to maintain their boundedness. It is necessary that a steering algorithm continue to operate in a sensible manner under these circumstances.

Near singular states, the linearization problem is not solvable as stated. The numerical difficulty that arises in computing the transformations is due to the fact that the matrix $A(x)$ in Eq. (24) is nearly singular. This matrix has the form

$$A(x) = \begin{bmatrix} A_1(x) & A_2(x) \\ 0 & I_{m-3} \end{bmatrix} \tag{42}$$

The MONITOR routine attempts to order the gimbal angles to guarantee numerical invertibility of $A_1(x)$; however, near a singular state, no such ordering exists. The matrix A_1 can be decomposed into

$$A_1 = V\Lambda V^T \tag{43}$$

where $\Lambda = \text{diag}[\lambda_1, \lambda_2, \lambda_3]$ is the diagonal matrix of eigenvalues of A_1, and $V = \text{col}[e_1, e_2, e_3]$ is the matrix whose columns are the orthonormalized eigenvectors. The problem of computing the linearizing feedback [Eq. (24)] can be transformed to the form

$$\begin{bmatrix} V^T & 0 \\ 0 & I_{m-3} \end{bmatrix} v = \begin{bmatrix} V^T \ddot{q} \\ \dot{z}_3 \end{bmatrix} = \begin{bmatrix} \Lambda V^T & V^T A_2 \\ 0 & I_{m-3} \end{bmatrix} [w(q, \theta) + u] \tag{44}$$

where the third row in the matrix on the right is nearly zero—assuming the eigenvalues decrease along the diagonal of Λ. Eliminating this row from the equation and increasing the dimension of the identity matrix by 1 yields the feedback transformation

$$u = \alpha(q, \theta) + \begin{bmatrix} \begin{bmatrix} -\lambda_1 e_1 - \\ -\lambda_2 e_2 - \end{bmatrix} & \begin{bmatrix} -e_1 - \\ -e_2 - \end{bmatrix} A_2 \\ 0 & I_{m-2} \end{bmatrix}^{-1} \begin{bmatrix} \begin{bmatrix} -e_1 - \\ -e_2 - \end{bmatrix} \ddot{q} \\ \dot{z}_3 \end{bmatrix} \tag{45}$$

Near a singular state, there is a direction about which the CMGs can produce no acceleration. This modification to the algorithm projects the desired acceleration onto the space orthogonal to the singular direction, and control of the spacecraft about the singular direction is replaced by an extra degree of gimbal freedom in the transformation. The spacecraft will not be controlled in the singular direction; however, control will be maintained along the other axes. Controllability will be recovered in the singular direction after the singular orientation has been eliminated. Depending on the torque and the orientation of the singular direction, the singularity may be a problem for only a very short time.

After the program resolves potential computational difficulties, the linearizing state and feedback transformations are evaluated in the routine TRANSFORMS. The routine CMG-DISTRIB is then called to compute the desired set of gimbal rates based on the current state of the CMG system. The routine APPROX calls the appropriate subroutines for formulating and solving the desired normed approximation problem. The 1- and 2-norm approximation problems are solved using the subroutines DLPRS and QPROG, respectively, from release 10.0 of the IMSL™ subroutine library. The ∞-norm approximation problem is solved using subroutine ZX3LP from release 9.2 of the IMSL™ library. The output of the steering program is a set of gimbal rates, u, which produce the commanded $\ddot{q}$ when possible.

This steering algorithm has been implemented as part of a simple rigid-body simulation of a spacecraft. It is assumed that there are no external torques and that the momentum state of the simulated spacecraft and the CMGs can be measured. The equations of motion are integrated using a fourth-order Runge-Kutta integration scheme. Before computing an integration step, a subroutine is called that can implement a variety of attitude control functions, and then the CMG steering algorithm is called. The chosen gimbal rates are then passed to a subroutine that executes a single integration step. The following section presents results from simulations using the program described in this section.

Simulation Examples

In this section, several simulations are presented to demonstrate the behavior of the proposed steering algorithm. The first example demonstrates the need for the fourth term in the rotation axis computation, [Eq. (39)]. This is an example of a situation in which the steering algorithm must deal explicitly with a problem that conventional gradient based methods would fail to recognize. The next example shows how the algorithm redistributes the CMG rotors when they are initialized in a singular configuration.

The inertia properties of the vehicle are listed in Table 1 and represent the rephased dual-keel space station after assembly sequence flight 7.[23] Attitude control torques are pro-

Table 1 Inertia properties for rephased, dual-keel space station

Inertia matrix, slug-ft^2		
2.425×10^7	-1.917×10^5	3.060×10^5
-1.917×10^5	3.556×10^6	2.333×10^5
3.060×10^5	2.333×10^5	2.515×10^7

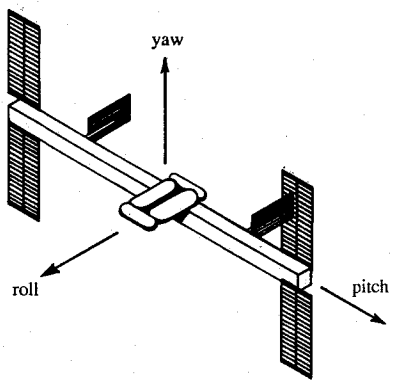

Fig. 4 Schematic of space station model.

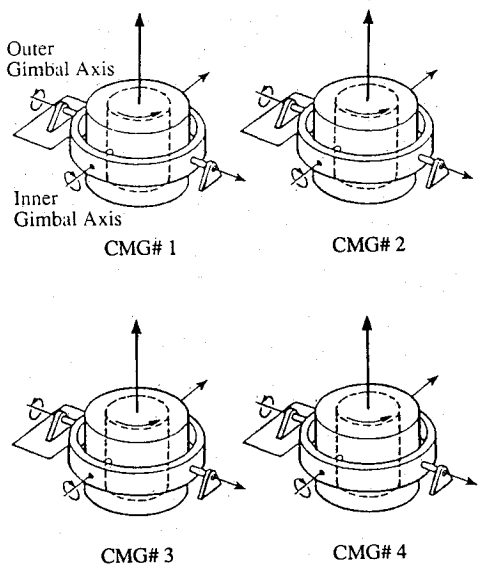

Fig. 5 Reference configuration for four parallel mounted CMGs.

vided by four parallel-mounted double-gimballed CMGs. In the parallel mount configuration, the outer gimbals are aligned with the vehicle pitch axis and the inner gimbals are aligned along roll. Each CMG rotor possesses 5000 ft-lb-s of angular momentum and can be gimballed about inner and outer mounts at peak rates of 5 deg/s. Inner gimbal displacements are limited to less than 90 deg and outer gimbals may rotate continuously. Figure 4 shows a schematic diagram of the vehicle along with the body reference frame, and the CMG mounting configuration is shown in Fig. 5. The set of constants used by the steering law to compute the desired gimbal rotation vectors are shown in Table 2. Although these simulations employ parallel CMG mounting, the structure of the steering law by no means requires this and is amenable to any mounting configuration.

In the first example, the CMG momentum vectors are initialized so that rotors 1 and 4 nearly align with the positive and negative yaw axes, respectively, and rotors 2 and 3 nearly align with the positive and negative roll axes, respectively. A constant torque of -100 ft-lb is commanded along the negative roll axis of the vehicle. This torque will cause the CMG rotors to align along the positive roll axis. The small initial gimbal offsets of ± 0.1 deg were used to maintain zero momentum and to insure that the desired rotation vector of rotor 3 consistently lies along its inner gimbal axis. As a consequence, this gimbal will eventually be rotated against its stop. The outer gimbal rotation term of Eq. (39) was added to the rotation vector computation to prevent this from happening. This problem is especially relevant to nonparallel mounting configurations where general spacecraft maneuvers are allowed.

Table 2 Constants used in rotation vector computation

Relative weights	Rotation vector constants
$k_1 = 0.2165$	—
$k_2 = 1.0$	$k_\tau = 1.57$
$k_3 = 1.0$	$k_1^{\text{inner}} = 0.0$ $k_2^{\text{inner}} = 0.6$
$k_4 = 1.0$	$k_1^{\text{outer}} = 0.6$ $k_2^{\text{outer}} = 0.7$

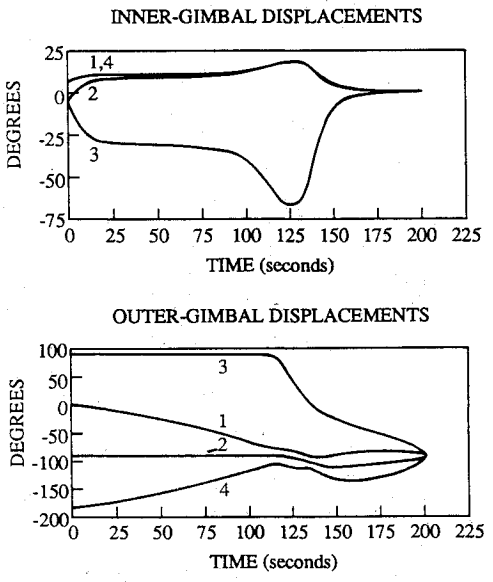

Fig. 6 Gimbal angles; momentum saturation along roll, 2 norm.

Figures 6 and 7 show the gimbal displacements and gimbal rates from the simulation. At about 125 s into the simulation, the outer gimbal of rotor 3 begins to rotate at its peak rate. Initially, the inner gimbal axis is aligned with the negative yaw axis of the vehicle. As the outer gimbal rotates, the inner gimbal axis eventually has a component along the positive yaw axis and the gimbal rate must change its sign to continue projecting more momentum in the positive roll direction. Throughout the simulated example, the commanded torque is maintained. Figure 8 shows that rotating the outer gimbal causes a drop in the gain function shortly before $t = 125$ s. Steering laws based on gain or controllability optimization would never choose to rotate the outer gimbal in this situation, and the inner gimbal would be forced against a stop. A similar statement applies to steering laws that attempt to avoid rotor line up. The approach[5] which keeps all inner gimbal angles equal, will not move rotor 3 from its initial position. While the technique can be modified to deal with this situation, it cannot be generalized to handle the arbitrary mounting configurations that might be used in a vehicle which is intended to undergo large-angle slewing maneuvers. Note

that in Fig. 7 the approximation algorithm is bounding the rate of outer gimbal 3 at its peak value.

In the second example, an angular rate change is commanded with the CMGs beginning in a configuration that is numerically singular in single precision on the computer being used. The attitude control law commands an angular acceleration proportional to a rate error in the pitch direction. The rotors are initialized in a zero momentum state with rotors 1 and 2 nearly aligned with the positive roll axis and rotors 3 and 4 nearly aligned with the negative roll axis; this configuration is numerically singular. The gimbal angle responses are shown in Fig. 9. The inner gimbals must project momentum along the positive pitch axis to achieve the rate change, but the outer gimbals move until they are evenly distributed about the net CMG momentum vector in order to alleviate the singular condition and attain a best orientation. In Fig. 10 the gain function is shown. The gain is initially almost zero and increases rapidly to about 80% of its maximum value (recall that gain is not being optimized). It then decreases as the CMGs must project momentum in the pitch direction to maintain the rate change. This example illustrates that the proposed algorithm functions in the vicinity of a singular state. Even if the requested torque had been along the singular direction, null motions would drive the rotors to a configuration which could produce the desired torque. Since most approaches to CMG steering impose gimbal rate limits by scaling the computed rates, they may command very small gimbal rates near a singular configuration. In contrast, the algorithm described here will command the maximum possible rates to obtain a more controllable configuration.

Conclusions

This paper has presented an approach to obtaining gimbal rates for the control of CMG-equipped spacecraft. A feedback linearizing transformation was used to linearize the spacecraft dynamics, and then the transformation's special form was exploited to obtain a normed approximation problem that controls the spacecraft in a commanded way while redistributing the gimbals in a desired direction. An algorithm for computing a desired set of gimbal rates was proposed for systems of double-gimbal CMGs and demonstrated with two examples in which many existing algorithms are known to fail.

Using the proposed approach, the problem of developing a steering law involves designing an algorithm for the computation of desired gimbal rates. This is conceptually simpler than having to determine a function whose gradient produces desired rates. A difficulty encountered with algorithms that seek local optima of functions is that these algorithms can get stuck in a locally optimal configuration. For the parallel mount configuration of four CMGs, the technique demonstrated here steers to a unique, stable, controllable configuration for the rotors, provided that the CMGs project momentum in either the roll or the yaw direction (the place-

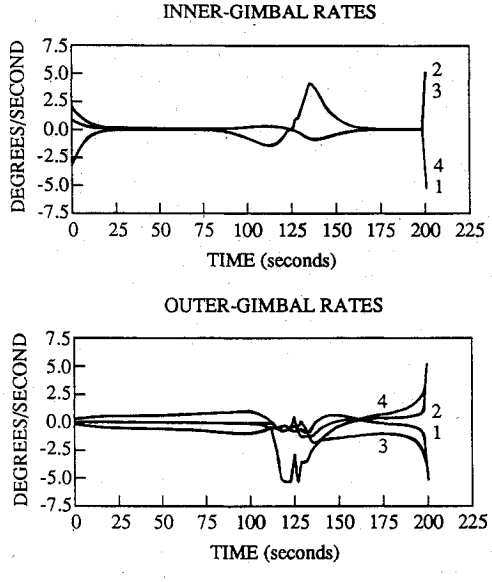

Fig. 7 Gimbal rates; momentum saturation along roll, 2 norm.

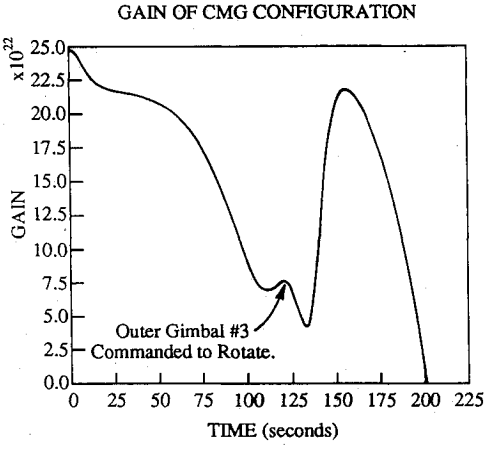

Fig. 8 Gain function during momentum saturation along roll, 2 norm.

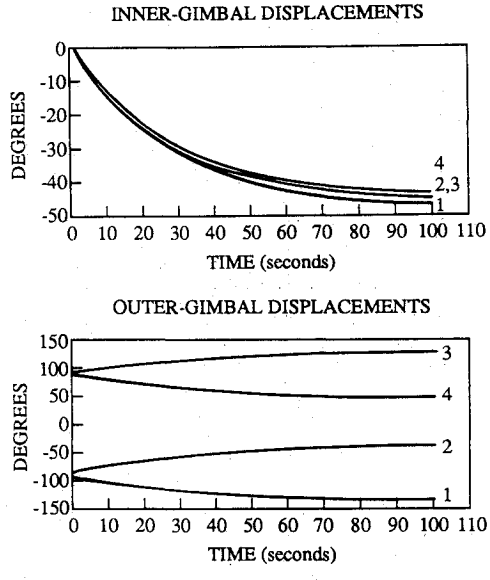

Fig. 9 Gimbal angles; rate change along pitch, 2 norm.

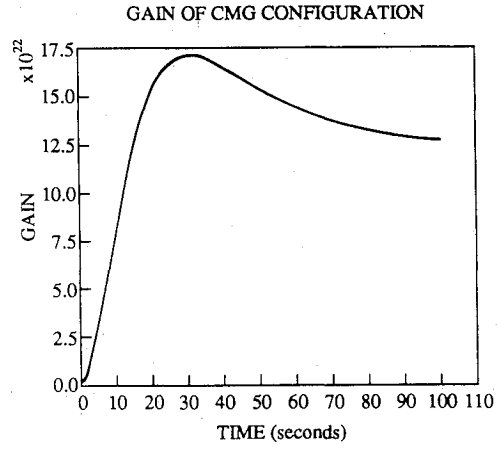

Fig. 10 Gain function during momentum saturation along pitch, 2 norm.

ment of the rotors is unique, not the location of the rotors by index). If the CMGs project momentum only in the pitch direction, the stable configuration can be rotated as a whole about the outer gimbal.

Most steering algorithms that have been proposed use the pseudoinverse of the matrix $\boldsymbol{D}\boldsymbol{h}_{\text{cmg}}$ to determine a torque producing set of gimbal rates. Because of the special form of the matrix $A(x)$ in Eq. (24), the computation of the linearizing transformation requires about the same numerical effort. This transformation can also be used as part of an attitude control law. Because the linearizing transformation developed here satisfies a torque constraint implicity, the feedback transformation can be incorporated into an existing steering algorithm (e.g., Ref. 1) to reduce the number of free variables that must be considered by three. Note that the technique for steering described in this paper could be implemented by parameterizing the null space of the gimbal rate vector and then solving a pseudoinverse problem. The reader would find that the resulting algorithm would be the same, except that the orthogonalization procedure to generate a basis for the null space would represent additional computations over the proposed method.

Although the technique proposed here is generally applicable to steering single-gimbal CMGs, the problem of determining desired rates is considerably more complicated. It may be necessary to relax constraints on the spacecraft control to insure adequate singularity avoidance capability. This problem should be a subject for continuing research.

Acknowledgment

This work was performed under NASA Contract NAS9-17560. Publication of this paper does not constitute approval by NASA of the findings or conclusions contained herein.

References

[1]Yoshikawa, T., "A Steering Law for Three Double-Gimbal Control Moment Gyro Systems," NASA TM-82390, Jan. 1981.

[2]Paradiso, J., "A Highly Adaptable Steering/Selection Procedure for Combined CMG/RGS Spacecraft Control," *Ninth Annual AAS Guidance and Control Conference*, AAS Paper 86-036, Jan. 1986.

[3]Kurokawa, K., Yajima, N., and Usui, S., "A New Steering Law of a Single-Gimbal CMG System of Pyramid Configuration," *10th IFAC Symposium on Automatic Control in Space*, 1981.

[4]Cornick, D., "Singularity Avoidance Control Laws for Single Gimbal Control Moment Gyros," AIAA Paper 79-1698, Aug. 1979.

[5]Kennel, H., "Steering Law for Parallel Mounted Double-Gimballed Control Moment Gyros," Rev. A, NASA TM-82390, Jan. 1981.

[6]Bedrossian, N., "Steering Law Design for Redundant Single Gimbal Control Moment Gyro Systems," S. M. Thesis, Mechanical Engineering Dept., Massachusetts Inst. of Technology, Cambridge, MA, 1987.

[7]Nakamura, Y., and Hanafusa, H., "Inverse Kinematic Solutions with Singularity Robustness for Robot Manipulator Control," *Journal of Dynamic Systems, Measurement, and Control*, Vol. 108, 1986, pp. 163–171.

[8]Branets, et al., "Development Experience of the Attitude Control System using Single-Axis Control Moment Gyroscopes for Long-Term Orbiting Space Stations," 38th Congress of the International Astronautical Federation, IAF Paper 87-04, Oct. 1987.

[9]Kennel, H., "A Control Law for Double-Gimballed Control Moment Gyros Used for Space Vehicle Attitude Control," NASA, 1970.

[10]Architectural Control Document: Guidance, Navigation, and Control System, Space Station Program Office, NASA, ACD 3/JSC 30259, Jan. 1987.

[11]Hunt, L., and Su, R., "Local Tranformations for Multi-Input Nonlinear Systems," *Joint Automatic Control Conference*, Paper FA-313, 1981, pp. 24–31.

[12]Jakubczyk, B., and Respondek, W., "On Linearization of Control Systems," *Bulletin Academie Polonaise des Sciences. Serie des Sciences Mathematiques, Astronomiques, et Physiques*, Vol. 28, 1980, pp. 517–522.

[13]Dzielski, J., "A Feedback Linearization Approach to Spacecraft Control Using Momentum Exchange Devices," Ph.D. Thesis, Mechanical Engineering Dept. Massachusetts Inst. of Technology, Cambridge, MA, 1988.

[14]Dwyer T., "Exact Nonlinear Control of Large Angle Rotational Maneuvers," *IEEE Transactions on Automatic Control*, Vol. 29, No. 9, 1984, pp. 769–774.

[15]Dwyer, T., "Exact Nonlinear Control of Spacecraft Slewing Manuevers with Internal Momentum Transfer," *Journal of Guidance, Control, and Dynamics*, Vol. 9, No. 2, 1986, pp. 240–247.

[16]Applegate, J., McMillion, J., and Smith, R., "Design and Operation of the Skylab Attitude and Pointing Control System," *Advances in the Astronautical Sciences*, Vol. 31 (Preprint), 1975.

[17]Brand, L., *Vector and Tensor Analysis*, Wiley, New York 1947.

[18]Brunovsky, P., "A Classification of Linear Controllable Systems," *Kybernetika*, Vol. 6, 1970, pp. 173–188.

[19]Wismer, D., and Chattergy, R., *Introduction to Nonlinear Optimization: A Problem Solving Approach*, North-Holland, New York, 1978.

[20]Fisher, W., "A Note on Curve Fitting with Minimum Deviations by Linear Programming," *Journal of the American Statistical Association*, June 1961, pp. 359–362.

[21]Kelley, J., "An Application of Linear Programming to Curve Fitting", *J. Soc. Indust. Appl. Math.*, Vol. 6, 1958, pp. 15–22.

[22]Wie, B., and Barba, P., "Quaternion Feedback for Spacecraft Large Angle Maneuvers," *Journal of Guidance, Control, and Dynamics*, Vol. 8, No. 3, 1985, pp. 360–365.

[23]Macloed, T., Rigsby, K., and Friedman, M., "Rephased Dual Keel Mass Properties and TEA Analysis," Lockheed Engineering Services Co., Houston, TX, Aug. 1986.